Asian Journal of Chemistry; Vol. 38, No. 11 (2026), 3029-3039
ASIAN JOURNAL OF CHEMISTRY
https://doi.org/10.14233/ajchem.2026.36716

Assessment of Groundwater Fluoride Contamination and Its Removal using Chemically Activated Agricultural Waste-Based Adsorbents

MANSHI AHLAWAT, DHARAMPAL SINGH*, and RONAK JAIN

School of Earth Science, Banasthali Vidyapith, Banasthali-304022, India

*Corresponding author: E-mail: dharam08@gmail.com

Received: 28 June 2026 *Accepted*: 12 October 2026 *Published online*: 13 November 2026 AJC-22534

Groundwater is the primary source of drinking water in rural areas, but fluoride contamination poses significant health risks when present above permissible limits. This study investigates the sustainable removal of fluoride using activated carbon (AC) derived from agricultural wastes, namely rice husk (RH) and potato peel (PP), activated with phosphoric acid. Batch adsorption experiments were carried out using synthetic fluoride solutions and groundwater collected from hand pumps and tube wells in the Banasthali (Niwai) region of Rajasthan. Fluoride concentrations in the groundwater ranged from 0.10 to 5.71 mg/L, with several samples exceeding the permissible limit of 1.5 mg/L. RH-AC achieved a maximum fluoride removal of 79%, compared with 54.17% for PP-AC at an initial fluoride concentration of 5 mg/L. The adsorption behaviour was best fitted by the Freundlich isotherm, while the pseudo-second-order model provided the best fit for the adsorption kinetics. The findings identify rice husk-based activated carbon (RH-AC) as a promising, low-cost adsorbent for fluoride removal from contaminated water. Using agricultural waste for this purpose may offer a practical route to water treatment while supporting SDGs 3 (Good Health and Well-being), 6 (Clean Water and Sanitation) and 12 (Responsible Consumption and Production).

Keywords: Fluoride contamination, Banasthali, Groundwater quality, Agricultural waste, Rice husk, Potato peel, Adsorption.

INTRODUCTION

Access to safe drinking water remains a major global concern, even though water covers a large part of the Earth's surface. Groundwater accounts for only about 0.6% of the Earth's total water reserves but provides drinking water to nearly half of the global population. Its role is particularly important in developing countries such as India, where it meets approximately 80% of rural drinking water needs and 50% of irrigation demand [1]. Rapid urbanization, industrial growth and population expansion have increased pressure on groundwater resources and contributed to contamination, posing risks to both human health and the environment.

Fluoride (F^-) is a common groundwater contaminant reported in more than 25 countries, with concentrations often exceeding the World Health Organization (WHO) guideline value of 1.5 mg/L [2]. Fluoride at low concentrations supports dental and skeletal health, while prolonged exposure to excessive levels can cause dental and skeletal fluorosis, renal dysfunction and neurological disorders [3-5]. Its presence in groundwater is linked to natural geological processes and human activities, making effective removal important for protecting public health.

Several treatment methods are available for fluoride removal such as reverse osmosis, ion-exchange, membrane filtration, electrochemical treatment and chemical precipitation [6]. Their use may be restricted by high operating costs and the need for specialized equipment and infrastructure. Adsorption is a practical alternative due to its simple operation, relatively low cost and potential for efficient fluoride removal [7,8]. Activated carbon (AC) is widely studied for this purpose, as its porous structure and large surface area provide sites for contaminant uptake [9,10].

Growing interest in sustainable treatment materials has encouraged the use of agricultural residues as precursors for activated carbon. Rice husk (RH) and potato peel (PP) are readily available byproducts that can be converted into useful adsorbents. Rice husk is abundant in rice-producing regions and offers a low-cost raw material with a stable structure [11]. Potato peel is generated in substantial quantities during potato processing and household food preparation. Its disposal presents a waste-management challenge, while its use as an ads-

This is an open access journal, and articles are distributed under the terms of the Attribution 4.0 International (CC BY 4.0) License. This license lets others distribute, remix, tweak, and build upon your work, even commercially, as long as they credit the author for the original creation. You must give appropriate credit, provide a link to the license, and indicate if changes were made.

orbent offers an opportunity to recover value from this residue [12].

Although rice husk- and potato peel-derived activated carbons prepared using phosphoric acid (H_3PO_4) have been investigated separately, their comparative performance for fluoride removal under identical experimental conditions remains insufficiently explored. This study addresses this gap by comparing the two bioadsorbents in terms of fluoride-removal efficiency, adsorption capacity, physico-chemical properties, equilibrium behaviour and adsorption kinetics. The comparison helps identify differences in adsorption capacity, equilibrium behaviour and fluoride removal efficiency between the two adsorbents.

Furthermore, the study assesses fluoride occurrence in drinking-water sources collected from hand pumps and tube wells in the Banasthali (Niwai) region of Rajasthan, India, linking a site-specific groundwater-quality concern with the laboratory evaluation of potential treatment materials. This approach supports further research into agricultural-waste valorization and fluoride-contaminated water treatment, contributing to the objectives of SDG 6 (clean water and sanitation), SDG 12 (responsible consumption and production) and SDG 3 (good health and well-being). However, the findings represent laboratory-scale evidence and require further validation before practical or large-scale application can be established.

EXPERIMENTAL

Study area: Niwai Tehsil is located in Rajasthan, south of Tonk district, and is surrounded by Ajmer, Bhilwara and Bundi districts. The area is connected to Jaipur by road, with the district headquarters approximately 167 km away. The region lies at an average elevation of about 296 m above mean sea level and covers approximately 153,969 hectares. The geographic location of Niwai is 25º35′ N 73º37′ E, 25.58º N 73.62º E. It is 296 m (971 feet) above mean sea level on average. The land-scape near Bisalpur Dam consists of relatively level terrain interspersed with hills and the area experiences a hot, arid climate. The present study investigates groundwater quality in fluoride-affected areas of Niwai Tehsil (Fig. 1), with particular attention to identifying locations where fluoride concentrations fall within acceptable limits. The findings are intended to improve understanding of local groundwater quality and support the selection of suitable water sources. The study may further guide the development

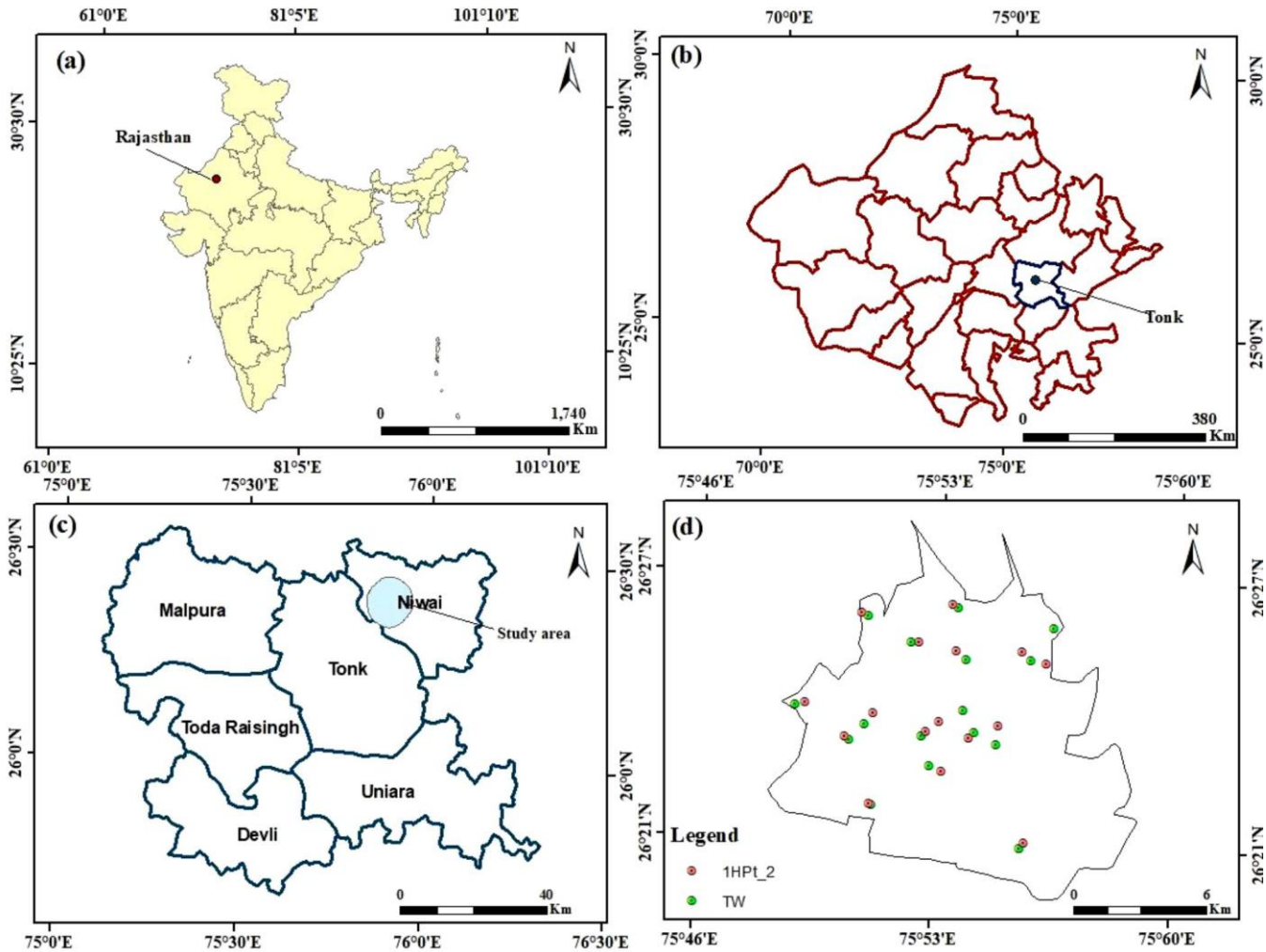


Fig. 1. Geospatial map of five km. nearby Banasthali villages, Tonk, Rajasthan, (a): India, (b) Rajasthan, (c): Tonk district and (d) sample study area); (source: Diva GIS and Survey of India)

of practical, low-cost and efficient defluoridation methods for village level applications.

Estimation of F^- in drinking water: Groundwater samples were collected from hand pumps (HP) and tube wells (TW) across 16 villages within a 5 km radius of Banasthali, Niwai, Rajasthan, using a random sampling method. The sampling area was defined with reference to the central point of Banasthali. After collection, the samples were stored at 4 ºC until laboratory analysis. Fluoride (F^-) concentrations were measured using a fluoride ion-selective meter. A 1000 ppm fluoride standard solution was prepared using distilled Milli-Q water and TISAB III buffer. Before sample analysis, the meter was calibrated using fluoride standards of 0.1, 1.0, 10 and 100 ppm. For calibration, 50 mL of each standard solution was mixed with 5 mL of TISAB III and the electrode was immersed until the reading stabilized. The electrode was rinsed thoroughly with distilled water between measurements. Groundwater samples were analyzed using the same procedure, with 50 mL of each sample mixed with 5 mL of TISAB III before measuring the fluoride concentration.

Preparation of activated carbon: Rice husk (RH) and potato peel (PP) were washed thoroughly with distilled water to remove surface contaminants and dried in a hot-air oven at 100 ºC for 6 h. The dried materials were carbonized in a muffle furnace at 300 ºC for 1 h and allowed to cool to room temperature for 30 min. The carbonized samples were then soaked in distilled water containing 75 mL of conc. H_3PO_4 in 500 mL beakers for 24 h to facilitate activation and improve porosity. Following activation, the materials were heated at 500 ºC. The samples were then treated with 100 mL of distilled water containing 0.5 g of $NaHCO_3$ to neutralize the residual phosphoric acid. The materials were washed initially with boiling water, followed by four to five rinses with distilled water until a neutral pH was attained. The washed samples were dried again at 100 ºC and sieved to obtain a uniform particle size of 1.18 mm. The prepared activated carbons were stored in clean, dry containers until further use [13].

Batch adsorption experiment: A fluoride stock solution with an initial concentration of 5 mg L^{-1} was prepared by diluting a 1000 mg L^{-1} fluoride standard solution with distilled water. Batch adsorption experiments were carried out to assess the fluoride removal performance of the prepared activated carbons. The effects of adsorbent dosage, contact time, solution pH and initial fluoride concentration were examined under controlled conditions. The effect of adsorbent dosage was evaluated using 2, 4, 6, 8 and 10 g of activated carbon with a uniform particle size of 1.18 mm. Each experiment was conducted by adding the specified adsorbent mass to 100 mL of fluoride solution (5 mg L^{-1}) in a conical flask. Contact time was investigated by agitating the mixtures for 30, 60, 90 and 120 min. The effect of pH was studied at values of 2, 4, 6, 8 and 10, adjusted using 0.1 N HNO_3 and 0.1 M NaOH. For these experiments, 10 g of RH-AC and 8 g of PP-AC were added separately to 100 mL of fluoride solution. The effect of initial fluoride concentration was examined over the range of 1.0-5.0 mg L^{-1} using fixed adsorbent doses of 10 g RH-AC and 8 g PP-AC. After adsorption, the residual fluoride concentration was measured to determine the removal efficiency by comparing the initial and equilibrium concentrations, as described in eqn. 1:

$$\text{Removal efficiency} = \frac{C_i - C_e}{C_i} \times V \quad (1)$$

where C_i represents the initial fluoride concentration, while C_e denotes the residual fluoride concentration at equilibrium; V refers to the total volume of the aqueous solution used in the experiment.

Adsorption isotherm: Isotherm modelling helps explain the adsorption behaviour of fluoride ions on adsorbent surfaces and their distribution between the solid and liquid phases at equilibrium. The Langmuir and Freundlich models are widely used in water and wastewater treatment to evaluate adsorption capacity and surface characteristics under constant temperature conditions [14]. The Langmuir model assumes adsorption on a uniform surface, whereas the Freundlich model accounts for surface heterogeneity and non-uniform adsorption energies [15]. The linear form of the Freundlich isotherm is expressed in eqn. 2:

$$\text{Log}(q_e) = \log K_f + \left(\frac{1}{n}\right)\log C_e \quad (2)$$

In the Freundlich model, K_f represents the adsorption capacity, while n describes the adsorption intensity and the favourability of the adsorption process. The Langmuir isotherm describes adsorption as a monolayer process occurring on a finite number of uniform adsorption sites on the adsorbent surface [16]. The linear form of the Langmuir equation is given in eqn. 3:

$$\frac{C_e}{q_e} = \frac{1}{K_l q_{max}} + \frac{1}{q_{max}} C_e \quad (3)$$

where K_l (L mg^{-1}) represents the Langmuir constant, which indicates the strength of interaction between the adsorbent and F^- ions, while q_{max} (mg g^{-1}) denotes the highest adsorption capacity corresponding to a complete monolayer on the adsorbent surface; C_e (mg L^{-1}) is the concentration of F^- remaining in the solution once equilibrium is reached and q_e (mg g^{-1}) refers to the amount of F^- adsorbed per gram of adsorbent under equilibrium conditions.

Kinetic isotherm: The rate constants for the pseudo-first-order (PFO) and pseudo-second-order (PSO) models were calculated from the experimental adsorption data collected at different contact times. The PFO model, originally proposed by Lagergren, was used to describe the adsorption kinetics. Its governing equation is presented in eqn. 4:

$$L_n(q_e - q_t) = \ln q_e - K_1 t \quad (4)$$

The equation for the PSO model, which describes equilibrium adsorption, was using eqn. 5 by [17]:

$$\frac{t}{q_t} = \frac{1}{K_2 q_e^2} + \frac{1}{q_e} t \quad (5)$$

where, t represents the contact time expressed in minutes. The parameter K_1 denotes the kinetic rate constant associated with the PFO model. The term q_t refers to the amount of adsorbate taken up by the adsorbent at any given time t, measured in mg g^{-1}, while q_e indicates the adsorption capacity

achieved at equilibrium. The constant K_2 corresponds to the rate constant of the PSO kinetic model and is expressed in g mg^{-1} min^{-1}.

Intra-particle diffusion model (IPD): The intraparticle diffusion (IPD) model, proposed by Weber and Morris, was used to investigate the diffusion mechanism involved in fluoride adsorption. The model relates the amount of fluoride adsorbed to the square root of contact time ($t^{1/2}$), as expressed in eqn. 6, to assess the role of intraparticle diffusion in the adsorption process.

$$q_t = K_{pi} t^{1/2} + C_i \quad (6)$$

where K_{pi} denotes the IPD rate constant, which quantifies the diffusion-controlled adsorption process and is measured in mg g^{-1} $min^{0.5}$.

RESULTS AND DISCUSSION

Fluoride (F^-) concentrations varied considerably across the 16 villages of Niwai Tehsil. The concentrations ranged from 0.14 to 5.71 mg L^{-1} in tube-well (TW) samples and from 0.10 to 4.86 mg L^{-1} in hand-pump (HP) samples. Villages near Banasthali generally recorded higher fluoride levels, whereas comparatively lower concentrations were observed near Niwai town. Site-specific fluoride concentrations are presented in Table-1 and their spatial distribution across the study area is illustrated in Fig. 2.

Several villages had fluoride concentrations exceeding the Central Pollution Control Board (CPCB) guideline of 1.0 mg L^{-1} for drinking water. The highest concentrations in HP samples were recorded at Monoharpura, Deori, Jagatpura, Ahmadpura, Banasthali, Shridaulatpura, Bhadagpura and Beedoli. In TW samples, increased concentrations were recorded at Deori, Jagatpura, Ahmadpura, Banasthali, Jagatpura Khurd, Shridaulatpura and Beedoli. These findings are important for rural communities that depend on groundwater for drinking, cooking, agriculture and livestock activities [18,19].

The higher fluoride concentrations observed in villages such as Shridaulatpura and Jagatpura may be related to differences in aquifer depth, local geological conditions and groundwater recharge patterns. Geological weathering and the dissolution of fluoride-bearing minerals are recognized sources of fluoride in groundwater. As groundwater moves through rocks and soil the gradual dissolution of fluoride-bearing minerals releases fluoride into the water and increases its concentration [20]. Differences in geological formations, recharge conditions and groundwater composition may explain the lower concentrations observed near Niwai town, although site-specific evidence is required to establish the causes of the spatial variation.

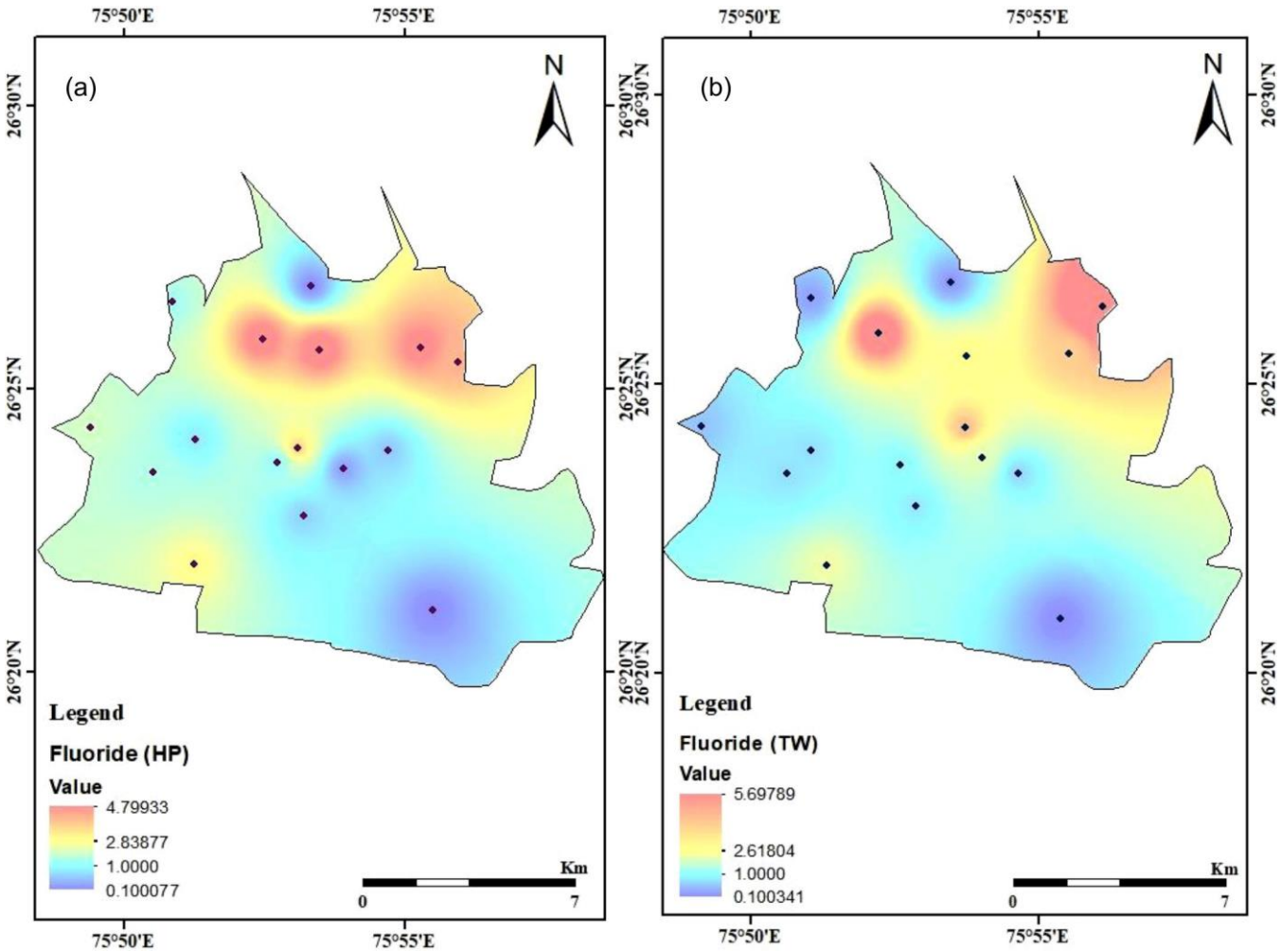


Fig. 2. Geospatial distribution of F^- concentration in the rural area, (a) TW and (b) HP

TABLE-1
FLUORIDE (F^-) CONCENTRATION LEVELS IN HAND-PUMP AND TUBE-WELL WATER SAMPLES COLLECTED FROM DIFFERENT VILLAGES IN THE STUDY AREA (mg L^{-1})

Location No.	Villages	Hand pump	Tube well	Location No.	Villages	Hand pump	Tube well
0	Niwai	0.1	0.1	8	Beedoli	4.5	5.7
1	Deori	2.9	2.4	9	Ahmadpura	3.8	3.2
2	Dangarthali	1.8	1	10	Shridaulatpura	4.8	2.7
3	Soorajpura	1.2	1	11	Khandewat	0.9	1.1
4	Monoharpura	2.2	0.7	12	Banasthali	3.4	3.4
5	Bhadagpura	1.7	0.3	13	Ramjipura	1.5	1.3
6	Barh-pathrajkhurd	0.1	0.2	14	JagatpuraKhurd	0.3	2.2
7	Jagatpura	4.6	4.6	15	Palei	0.8	0.9

Characterization of activated carbons

Proximate analysis: The proximate analysis of activated carbons prepared from rice husk (RH-AC) and potato peel (PP-AC) demonstrated distinct physico-chemical properties (Table-2). PP-AC had a higher fixed carbon content (8.96%) than RH-AC (7.54%), which may reflect differences in their carbonization behaviour and could influence their adsorption performance. Fixed carbon content is an important parameter in assessing activated carbon quality [21]. RH-AC had a higher bulk density (4.87 g cm^{-3}) than PP-AC (3.49 g cm^{-3}). The lower bulk density of PP-AC may be associated with a more open structure that can favour adsorption although porosity measurements are needed to confirm this interpretation [17]. The pH values of RH-AC (5.63) and PP-AC (5.04) indicate mildly acidic surfaces that may affect the adsorption of metal ions and organic contaminants through interactions with surface charge [22].

TABLE-2
PROXIMATE DATA OF AGRICULTURE WASTE DERIVED ACTIVATED CARBON

Proximity analysis	Rice husk	Potato peel
Moisture analysis (MC)	4.18	9.71
Volatile matter (VM)	25.33	28.11
Ash content (AC)	62.95	71.16
Fixed carbon (FC)	7.54	8.96
Bulk density	4.87	3.49
pH	5.63	5.04

FTIR spectra analysis: The FTIR spectra of RH-AC and PP-AC showed broad bands at 3805-3676 cm^{-1} assigned to –OH stretching vibrations of hydroxyl groups. Bands in the 3439-2523 cm^{-1} region were attributed to cellulose and hemicellulose components. The peaks at 3301, 3060, 2943 and 2884 cm^{-1} were assigned to aliphatic C–H stretching vibrations [23]. The band at 1618 cm^{-1} was associated with C=O stretching in carbonyl groups while the peak near 1590 cm^{-1} was attributed to aromatic C=C/C=O vibrations. Peaks at 1288 and 1115 cm^{-1} corresponded to C–O and C–O–C stretching vibrations in cellulose-like structures (Figs. 3a and 3c). Bands within 1300-900 cm^{-1} were attributed to phosphorus containing groups such as P=O and P–O–C linkages introduced during H_3PO_4 activation [24,25]. Strong bands near 1097 and 808 cm^{-1} were assigned to asymmetric and symmetric Si–O stretching vibrations respectively [26]. These oxygen-, phosphorus- and silicon-containing groups may provide active sites for fluoride adsorption and influence the surface chemistry of both adsorbents.

The FTIR spectra of RH-AC and PP-AC after fluoride adsorption show changes in the position and intensity of several absorption bands compared with the chemically modified adsorbents (Figs. 3b and 3d). These changes suggest the involvement of surface functional groups in fluoride binding. The broad bands in the region of 3805-3676 cm^{-1} are related to the –OH stretching vibrations and changes in this region may indicate the participation of hydroxyl groups in the adsorption process. Variations in the bands assigned to C–O and C–O–C vibrations near 1288 and 1115 cm^{-1} suggest possible interactions involving oxygen-containing surface groups. Changes in the bands associated with P–O and P–O–C linkages in the 1300-900 cm^{-1} region may reflect the contribution of phosphorus containing groups to fluoride uptake. The bands near 1097 and 808 cm^{-1}, assigned to Si–O stretching vibrations, may indicate the involvement of silicon-containing surface sites. These spectral changes suggest that fluoride adsorption may involve interactions with hydroxyl and other oxygen-containing groups, along with phosphorus- and silicon-containing sites.

SEM: The SEM micrographs of rice husk-based activated carbon (RH-AC) and potato peel-based activated carbon (PP-AC) before and after fluoride treatment are shown in Fig. 4. Before treatment (Fig. 4a and c) the adsorbents showed rough and irregular surfaces with well-developed pores following carbonization and chemical activation using H_3PO_4 and $NaHCO_3$ at 500 ºC. These surface features provide potential sites for fluoride adsorption. After treatment with fluoride contaminated water (Fig. 4b and d) the surfaces appeared smoother with partial pore blockage and visible deposits. These changes suggest that fluoride adsorption altered the surface morphology and may have occupied some of the accessible pores.

X-ray diffraction (XRD): XRD analysis was used to examine the crystallinity and phase composition of the prepared materials (Fig. 5). The RH sample showed a broad diffraction peak at $2\theta \approx 24^{\circ}$, which was attributed to predominantly amorphous silica [21]. After chemical activation with H_3PO_4 and $NaHCO_3$ additional peaks appeared near 25º and 42º, which may indicate the development of partially ordered carbon structures. RH-AC and PP-AC exhibited more distinct diffraction features than the raw materials. A promi-

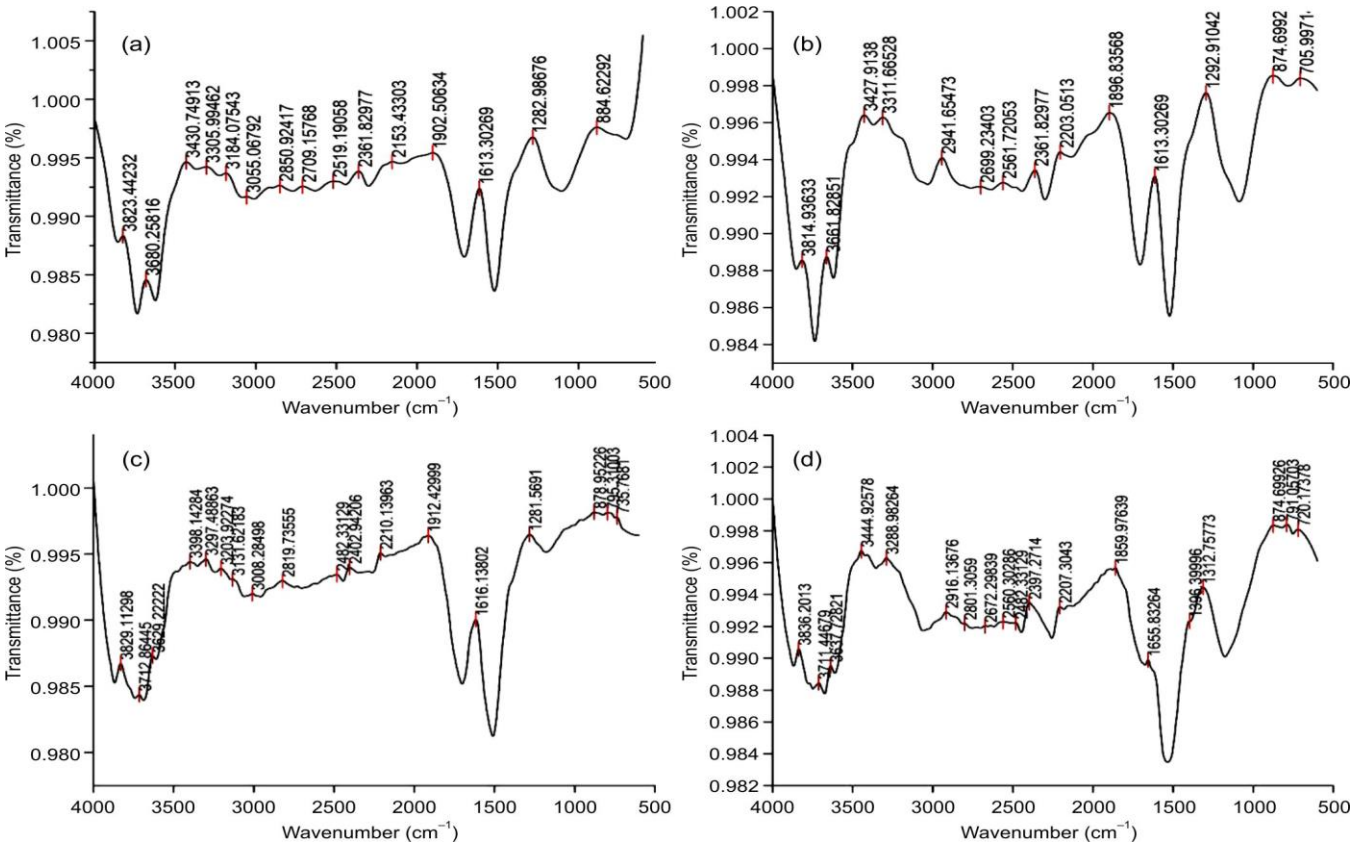


Fig. 3. FTIR spectra of agriculture-derived activated carbon before and after fluoride removal

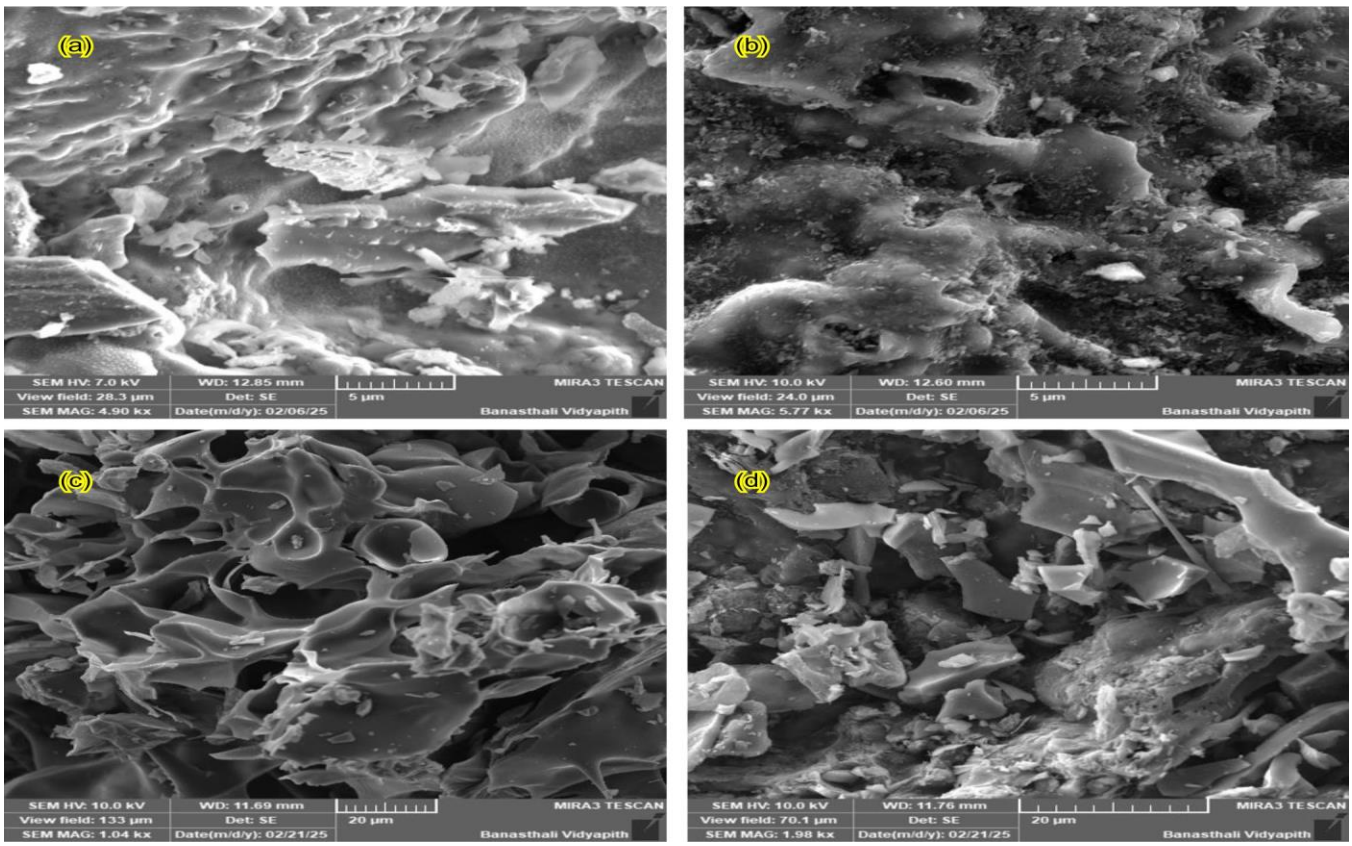


Fig. 4. SEM images of AC (a) chemically treated RH-AC (b) after water treatment RH-AC, (c) chemically modified PP-AC, (d) after water treatment PP-AC

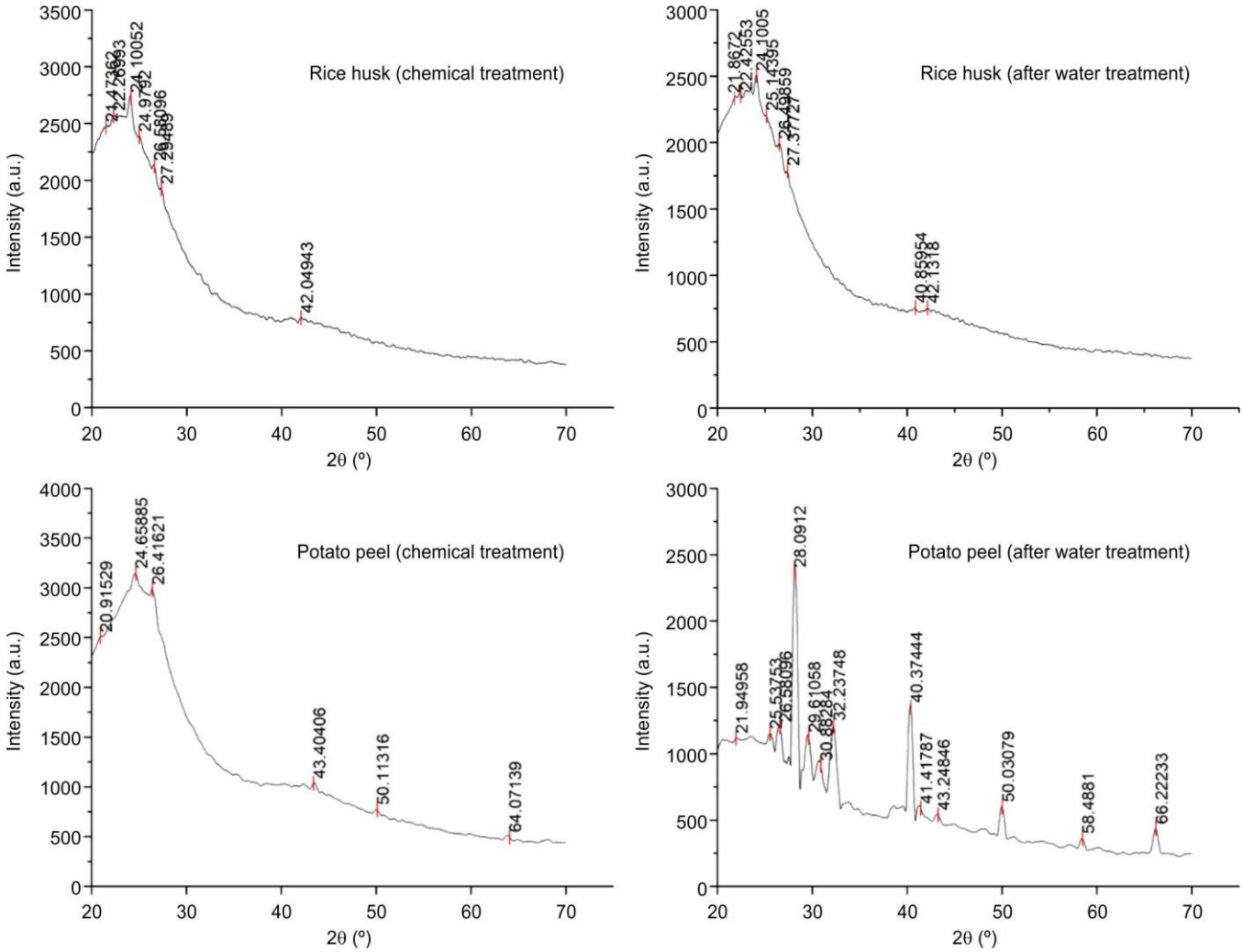


Fig. 5. XRD patterns of agriculture derived- AC before and after fluoride adsorption

nent peak at 2θ = 26.6º was assigned to the (002) plane of graphite [27] while the reflection at 43.6º was associated with crystalline graphite in accordance with JCPDS No. 41-1487 [6]. A peak at 50.6º was attributed to a KCl phase. These diffraction features suggest differences in the structural ordering and phase composition of the prepared adsorbents.

Fluoride removal analysis: Adsorbent dosage influenced fluoride removal by RH-AC and PP-AC. As shown in the graph the removal efficiency of RH-AC increased from 39.0% at 2 g to 88.19% at 10 g per 100 mL. PP-AC achieved a maximum removal of 54.17% at 8 g per 100 mL with no further improvement at a higher dosage. The improved removal at higher dosages can be attributed to the availability of more adsorption sites. The decrease in PP-AC performance at 10 g may be related to particle aggregation and reduced access to active sites. These results show that the optimum dosage depends on the adsorbent and that increasing the material quantity does not always improve fluoride removal.

Although RH-AC achieved greater fluoride removal its high dosage requirement needs consideration when evaluating practical use. Removal efficiency represents the proportion of fluoride removed from water whereas adsorption capacity indicates the amount of fluoride retained per unit mass of adsorbent. Both parameters are important when comparing performance and estimating material requirements.

Effect of contact time: As the contact period increased from 30 to 120 min, the removal efficiency of RH-AC increases from 61.83% to 87.98% while PP-AC increased from 39.57% to 53.64% (Fig. 6a). Longer contact allows fluoride ions more time to interact with the adsorbent surface and move into accessible pores. Similar trends have been reported for fluoride adsorption by activated carbon-based materials [28,29].

Effect of pH: Solution pH affected the adsorption performance of both materials. The highest removal was observed at pH 8 (Fig. 6b), which may reflect favourable interactions between fluoride ions and the adsorbent surfaces under these conditions. At strongly acidic or alkaline pH values the surface charge and competition from other ions may reduce fluoride uptake. These findings are consistent with earlier studies reporting effective fluoride adsorption near neutral to slightly alkaline pH [30].

Effect of initial concentration: The initial fluoride concentration influenced the percentage removal and adsorption capacity. As the initial concentration increased from 1 to 5 mg L^{-1}, the removal efficiency decreased (Fig. 6c). At lower concentrations more adsorption sites were available relative

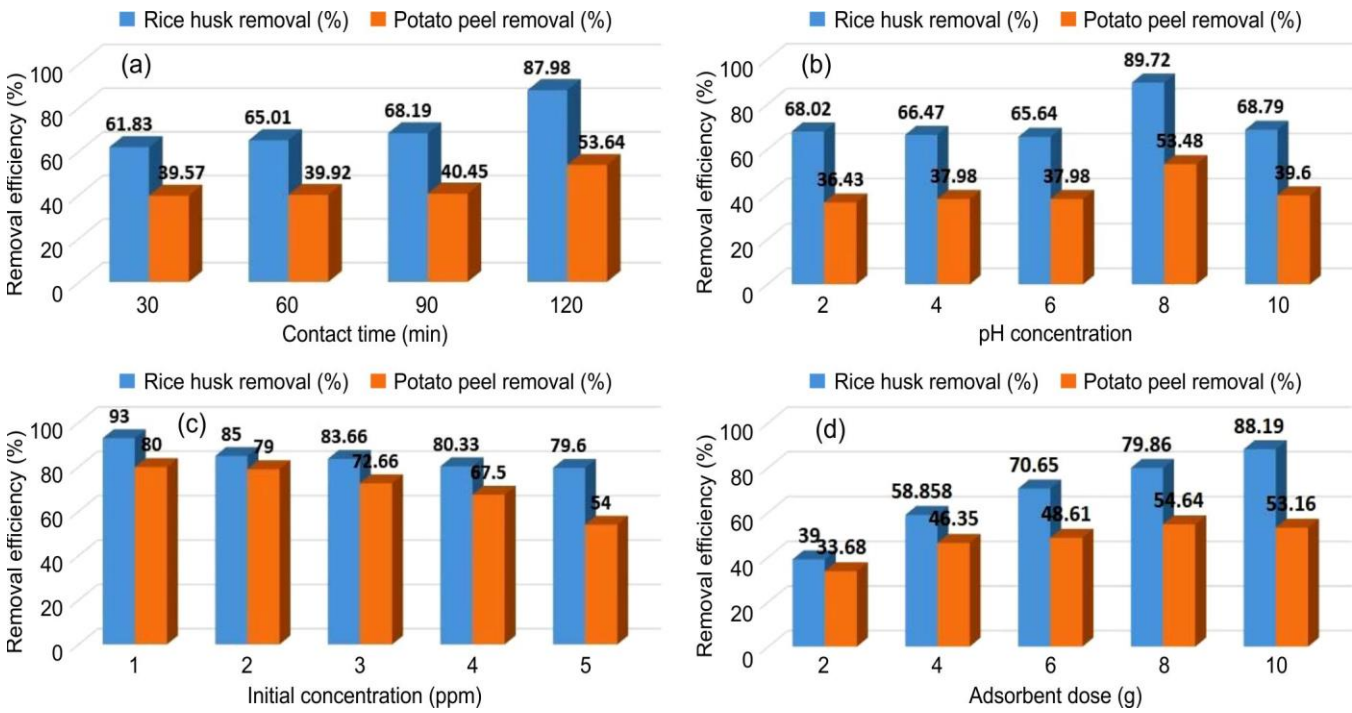


Fig. 6. Effect of (a) contact time, (b) solution pH, (c) initial fluoride concentration and (d) adsorbent dosage on fluoride (F^-) removal efficiency using rice husk-derived activated carbon (RH-AC) and potato peel-derived activated carbon (PP-AC) under batch adsorption conditions

to the number of fluoride ions in solution. At higher concentrations these sites became increasingly occupied. The higher concentration gradient can still promote mass transfer and increase the amount of fluoride adsorbed per unit mass even when the percentage removed decreases [28,31].

Effect of dosage: RH-AC performed better than PP-AC under the tested conditions. At an initial fluoride concentration of 5 mg L^{-1} RH-AC reduced the concentration to 0.68 mg L^{-1} at a dosage of 10 g per 100 mL (Fig. 6d). This corresponded to 88.19% removal and an equilibrium adsorption capacity of 0.0508 mg g^{-1}. PP-AC reduced the concentration from 5.76 to 2.64 mg L^{-1} at 8 g per 100 mL and achieved 54.17% removal with an adsorption capacity of 0.0390 mg g^{-1}. These results support the greater removal efficiency of RH-AC under the conditions tested. The relatively low adsorption capacities and high adsorbent dosages must be considered when assessing its practical potential.

Adsorption isotherm: Adsorption isotherms were analyzed to examine fluoride uptake by rice husk activated carbon (RH-AC) and potato peel activated carbon (PP-AC). Both isotherms showed a steep rise at low fluoride concentrations followed by a steady plateau as the concentration increased. The Langmuir model showed a moderate fit to the experimental data with R^2 values of 0.86 for RH-AC and 0.91 for PP-AC. The Freundlich model provided a better fit with R^2 values of 0.94 and 0.97 for RH-AC and PP-AC, respectively (Fig. 7). This better fit suggests that fluoride adsorption was more consistent with heterogeneous surface behaviour than with the assumptions of the Langmuir model. The Freundlich constants ($1/n < 1$) further indicate favourable adsorption. Similar trends have been reported for fluoride removal using activated carbon-based adsorbents [32,33].

Kinetic isotherms: Fluoride adsorption kinetics were examined using pseudo-first-order (PFO) and pseudo-second-order (PSO) models along with the intraparticle diffusion (IPD) model. The PSO model provided the best fit for both adsorbents with R^2 values of 0.92 for RH-AC and 0.89 for PP-AC compared with 0.69 and 0.85, respectively for the PFO model (Fig. 8). This suggests that the PSO model better describes the adsorption rate under the tested conditions although the model fit alone does not confirm chemisorption as the dominant mechanism. The IPD model indicated a contribution from diffusion during fluoride uptake. Its R^2 values of 0.89 for RH-AC and 0.56 for PP-AC suggest that intraparticle diffusion alone may not control the adsorption rate. Other processes such as surface adsorption and boundary-layer diffusion may contribute to fluoride removal [34,35].

Comparative studies: Table-3 compares the fluoride removal performance of rice husk activated carbon (RH-AC) and potato peel activated carbon (PP-AC) activated using orthophosphoric acid (H_3PO_4) and sodium bicarbonate ($NaHCO_3$) with that of other adsorbents reported in previous studies.

Applications: Fluoride removal from drinking water was evaluated using RH-AC and PP-AC at the optimum dosages identified in the batch experiments. RH-AC was applied at 10 g per 100 mL while PP-AC was used at 8 g per 100 mL with a contact time of 120 min. The initial and residual fluoride concentrations were measured using a fluoride ion-selective electrode. The water samples had a pH of 8.02. RH-AC showed better fluoride removal than PP-AC and performed more effectively in fulfilling the CPCB permissible limit for drinking water as shown in Fig. 9. These findings suggest that RH-AC and PP-AC have potential for fluoride removal

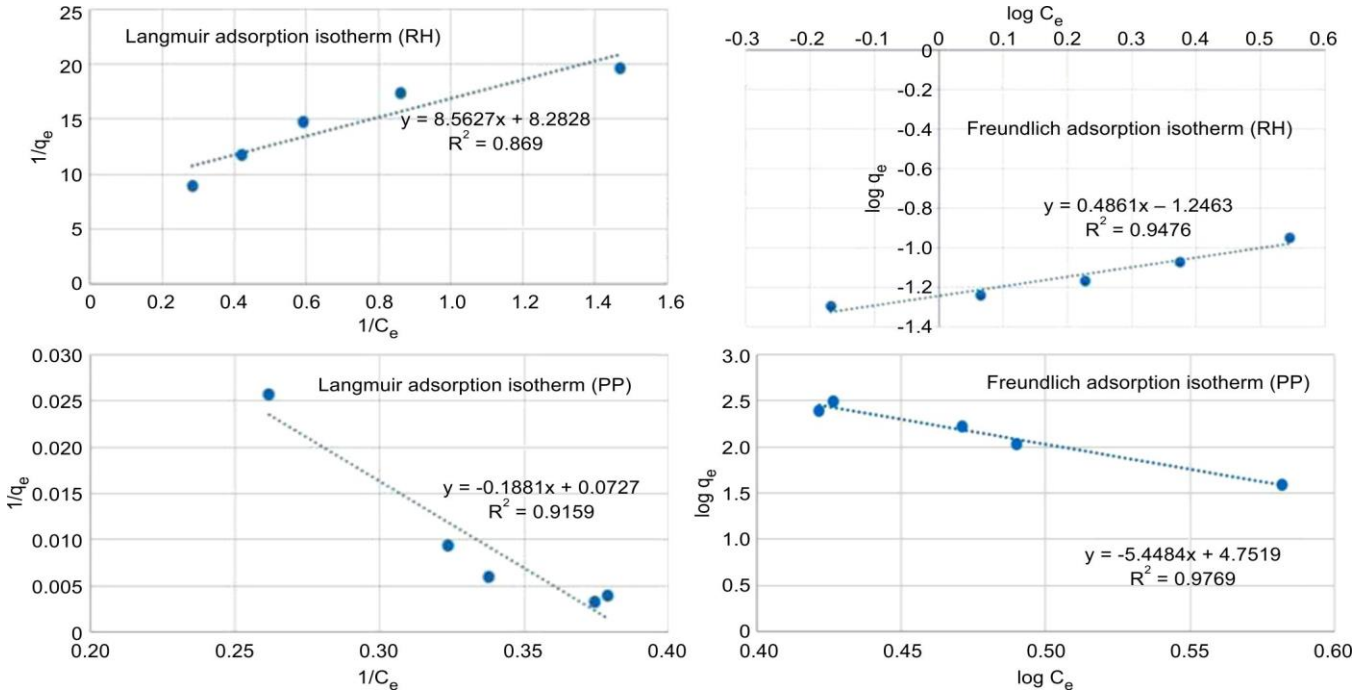


Fig. 7. Plots of different adsorption isotherm model for F^- removal using agriculture waste-derived AC

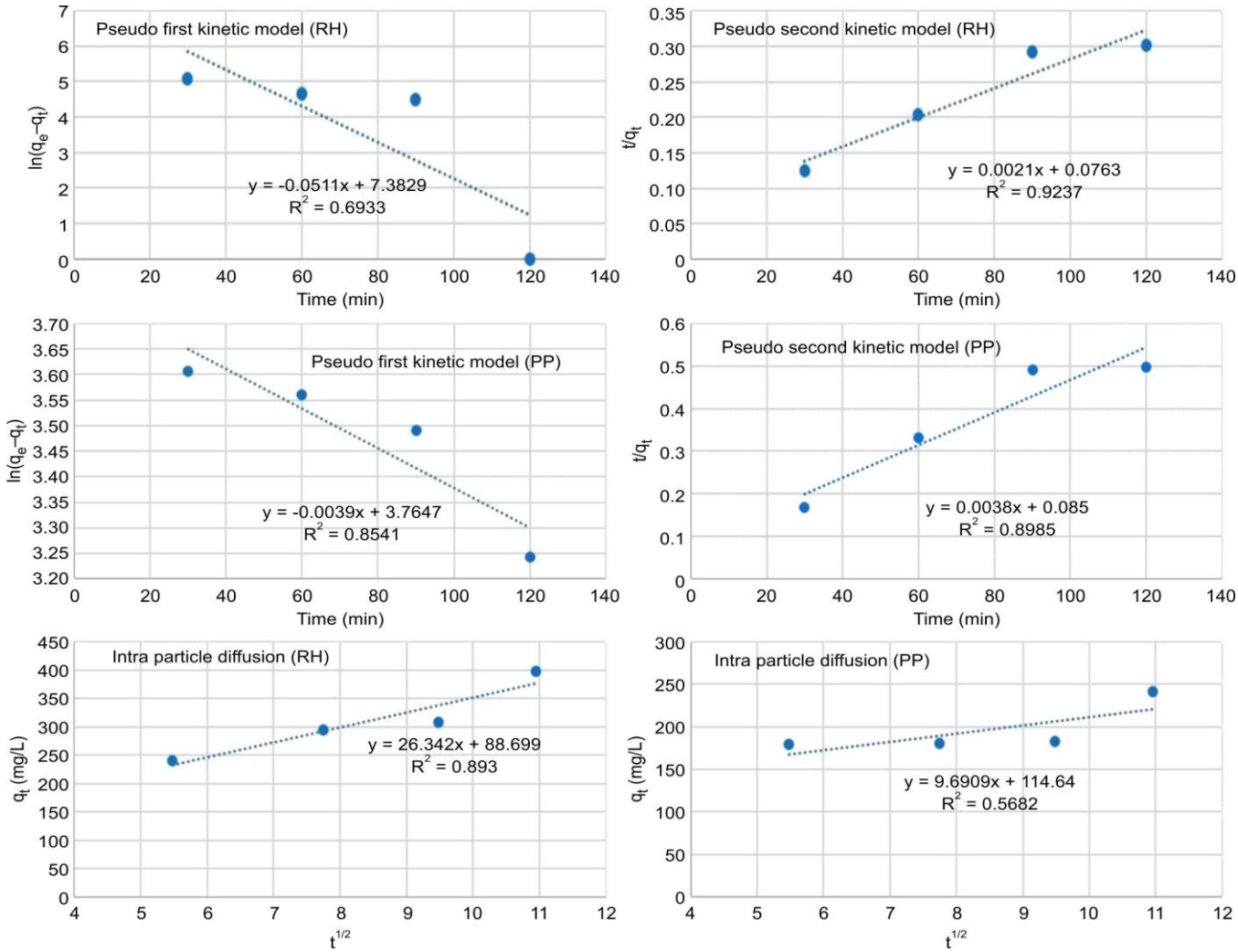


Fig. 8. Plots of different kinetic isotherm model for fluoride adsorption using agriculture waste-derived AC

TABLE-3
COMPARATIVE DATA OF FLUORIDE REMOVAL EFFICIENCY OF DIFFERENT ADSORBENTS UNDER VARIOUS EXPERIMENTAL CONDITIONS

Adsorbent	Initial conc. of F^- (mg L^{-1})	Removal (%) of F^-	Ref.
Sugarcane bagasse	4	45	[36]
Activated KOH-treated jamun seed	10	50	[37]
Bael (*Aegle marmelos*) shell-activated	8	46	[38]
Ficus benghalensis leaf	5	79	[39]
Coconut root	5	93	[40]
Tamarindus indica activated carbon	6	94	[41]
Rice husk-based nanocellulose	2	74	[42]
Rice husk	5	79	Present study
Potato peel	5	54	Present study

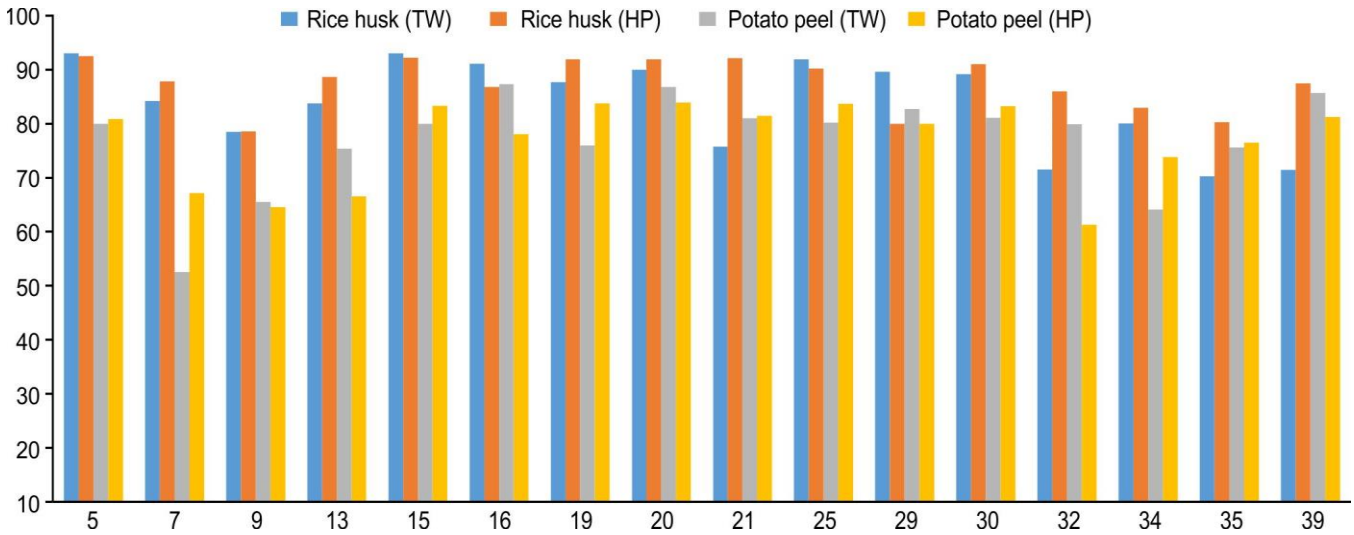


Fig. 9. Comparison of defluoridation efficiencies of rural groundwater samples using activated carbons derived from rice husk and potato peel under TW and HP conditions

from drinking water. Using agricultural residues as precursors for activated carbon can help reduce waste and support resource recovery. This approach is relevant to Sustainable Development Goals (SDGs) 3, 6 and 12, which address health and well-being, clean water and sanitation and responsible consumption and production. Rice husk and potato peel offer potential value as waste-derived adsorbent materials. Their practical affordability and reliability still require assessment of treatment performance, regeneration, processing costs and long-term use. Agricultural-waste-derived activated carbon has been investigated for removing water contaminants and may offer a useful approach to more sustainable water treatment.

Conclusion

This study investigated fluoride contamination in groundwater across 16 villages of Niwai Tehsil in Rajasthan and evaluated the fluoride removal performance of H_3PO_4- and $NaHCO_3$-modified activated carbons prepared from rice husk (RH-AC) and potato peel (PP-AC). Fluoride concentrations ranged from 0.14 to 5.71 mg L^{-1} in tube-well samples and from 0.10 to 4.86 mg L^{-1} in hand-pump samples. Several locations exceeded the CPCB guideline of 1.0 mg L^{-1} for drinking water, which highlights the urgent need for effective treatment in affected areas. RH-AC performed better than PP-AC under the tested conditions and achieved maximum fluoride removal efficiencies of 88.19% at 10 g per 100 mL and 54.17% at 8 g per 100 mL, respectively. A contact time of 120 min and a solution pH of 8 favoured fluoride removal. The Freundlich isotherm provided a better fit to the equilibrium data than the Langmuir model, while the pseudo-second order model best described the adsorption kinetics. The intraparticle diffusion contributed to fluoride uptake but was not the sole rate-controlling process. The study supports SDG 3, 6 and 12 through the use of rice husk and potato peel waste. Further studies on regeneration, real-water performance, scalability cost and environmental impact are required to establish their practical sustainability.

ACKNOWLEDGEMENTS

The authors sincerely extend their heartfelt gratitude to the Vice-Chancellor of Banasthali Vidyapith for relentless support, encouragement and the motivation during the course of this research work.

CONFLICT OF INTEREST

The authors declare that there is no conflicts of interest regarding the publication of this article.

DECLARATION OF AI-ASSISTED TECHNOLOGIES

During the preparation of this manuscript, the authors used an AI-assisted tool(s) to improve the language and no data, results or scientific conclusions were generated by AI. All analyses, interpretations and conclusions are the authors' own. The authors reviewed and edited the content and take full responsibility for the published work.

REFERENCES

1. R.T. Iwar, O.T. Iorhemen, K. Ogedengbe and K.K. Katibi, *Environ. Chem. Ecotoxicol.*, **3**, 142 (2021); https://doi.org/10.1016/j.enceco.2021.03.003
2. C.P. Ahada and S. Suthar, *Expo. Health*, **11**, 267 (2019); https://doi.org/10.1007/s12403-017-0268-4
3. A.L. Choi, G. Sun, Y. Zhang and P. Grandjean, *Environ. Health Perspect.*, **120**, 1362 (2012); https://doi.org/10.1289/ehp.1104912
4. K.Y. Foo and B.H. Hameed, *Chem. Eng. J.*, **156**, 2 (2010); https://doi.org/10.1016/j.cej.2009.09.013
5. M. Yousefi, S. Ghalehaskar, F.B. Asghari, A. Ghaderpoury, M.H. Dehghani, M. Ghaderpoori and A.A. Mohammadi, *Regul. Toxicol. Pharmacol.*, **107**, 104408 (2019); https://doi.org/10.1016/j.yrtph.2019.104408
6. A.I. Osman, J. Blewitt, J.K. Abu-Dahrieh, C. Farrell, A.A.H. Al-Muhtaseb, J. Harrison and D.W. Rooney, *Environ. Sci. Pollut. Res. Int.*, **26**, 37228 (2019); https://doi.org/10.1007/s11356-019-06594-w
7. I. Anastopoulos, A. Bhatnagar, B.H. Hameed, Y.S. Ok and M. Omirou, *J. Mol. Liq.*, **240**, 179 (2017); https://doi.org/10.1016/j.molliq.2017.05.063
8. N.P. Raval, P.U. Shah and N.K. Shah, *J. Environ. Manage.*, **179**, 1 (2016); https://doi.org/10.1016/j.jenvman.2016.04.045
9. M. Ergović Ravančić and M. Habuda-Stanić, *Water*, **16**, 3439 (2024); https://doi.org/10.3390/w16233439
10. Y. Sudaryanto, S. Hartono, W. Irawaty, H. Hindarso and S. Ismadji, *Bioresour. Technol.*, **97**, 734 (2006); https://doi.org/10.1016/j.biortech.2005.04.029
11. R.A. Fallahzadeh, M. Miri, M. Taghavi, A. Gholizadeh, R. Anbarani, A. Hosseini-Bandegharaei, M. Ferrante and G. Oliveri Conti, *Food Chem. Toxicol.*, **113**, 314 (2018); https://doi.org/10.1016/j.fct.2018.02.001
12. Y.S. Ho and G. McKay, *Chem. Eng. J.*, **70**, 115 (1998); https://doi.org/10.1016/S0923-0467(98)00076-1
13. S.K. Shukla, N.R.S. Al Mushaiqri, H.M. Al Subhi, K. Yoo and H. Al Sadeq, *Appl. Water Sci.*, **10**, 62 (2020); https://doi.org/10.1007/s13201-020-1145-z
14. M. Suneetha, B.S. Sundar and K. Ravindhranath, *J. Anal. Sci. Technol.*, **6**, 15 (2015); https://doi.org/10.1186/s40543-014-0042-1
15. S. Paudel and B. Shrestha, *Int. J. Adv. Social Sci.*, **3**, 27 (2020).
16. M. Ghorbani and H. Eisazadeh, *Iran. J. Energy Environ.*, **3**, 66 (2012); https://doi.org/10.5829/idosi.ijee.2012.03.01.3343.
17. O. Ioannidou and A. Zabaniotou, *Renew. Sustain. Energy Rev.*, **11**, 1966 (2007); https://doi.org/10.1016/j.rser.2006.03.013
18. V. Chaudhary and S. Satheeshkumar, *Appl. Water Sci.*, **8**, 218 (2018); https://doi.org/10.1007/s13201-018-0865-9
19. V. Srinivasan, N.R. Lakshmikantha, G. Manjunatha and G.N. Shinde, *PLOS Water*, **4**, e0000138 (2025); https://doi.org/10.1371/journal.pwat.0000138
20. N. Adimalla and H. Qian, *SN Appl. Sci.*, **1**, 202 (2019); https://doi.org/10.1007/s42452-019-0219-8
21. H. Marsh and F. Rodríguez-Reinoso, Elsevier Science & Technology Books (2006).
22. R.C. Bansal and M. Goyal, Activated Carbon Adsorption, CRC Press (2005).
23. M.J.C.R. Schwanninger, J.C. Rodrigues, B. Hinterstoisser and H. Pereira, *Vib. Spectrosc.*, **36**, 23 (2004); https://doi.org/10.1016/j.vibspec.2004.02.003
24. A.M. Puziy, O.I. Poddubnaya, A. Martínez-Alonso, F. Suárez-García and J.M. Tascón, *Carbon*, **43**, 2857 (2005); https://doi.org/10.1016/j.carbon.2005.06.014
25. M.S. Solum, R.J. Pugmire, M. Jagtoyen and F. Derbyshire, *Carbon*, **33**, 1247 (1995); https://doi.org/10.1016/0008-6223(95)00067-N
26. B.D. Mukri, K. Krushnamurty, A. Chowdhury, D. Suryakala and C. Subrahmanyam, *BioResources*, **11**, 9175 (2016).
27. C.N. Barnakov, G.P. Khokhlova, A.N. Popova, S.A. Sozinov and Z.R. Ismagilov, *Euras. Chem.-Technol. J.*, **17**, 87 (2015); https://doi.org/10.18321/ectj198
28. R. Maddalena, C. Hall and A. Hamilton, *Thermochim. Acta*, **672**, 142 (2019); https://doi.org/10.1016/j.tca.2018.09.003
29. M.A. Rahman, S. Bar and L. Parwani, *Mater. Today Proc.*, **68**, 1158 (2022); https://doi.org/10.1016/j.matpr.2022.09.323
30. B. Vijila, E.H. Edinsha Gladis, J. Michael Ahitha Jose, T.M. Sharmila and J. Joseph, *Mater. Today Proc.*, **45**, 2125 (2021); https://doi.org/10.1016/j.matpr.2020.09.729
31. M.G. Sujana, H.K. Pradhan and S. Anand, *J. Hazard. Mater.*, **161**, 120 (2009); https://doi.org/10.1016/j.jhazmat.2008.03.062
32. A. Amalraj and A. Pius, *Appl. Water Sci.*, **7**, 2653 (2017); https://doi.org/10.1007/s13201-016-0479-z
33. A.M. George and A.R. Tembhurkar, *Chin. J. Chem. Eng.*, **27**, 92 (2019); https://doi.org/10.1016/j.cjche.2018.03.004
34. S. Bakhta, Z. Sadaoui, N. Bouazizi, B. Samir, O. Allalou, C. Devouge-Boyer, M. Mignot and J. Vieillard, *RSC Adv.*, **12**, 2332 (2022); https://doi.org/10.1039/D1RA08209D
35. R.I. Yousef, B. El-Eswed and A.H. Al-Muhtaseb, *Chem. Eng. J.*, **171**, 1143 (2011); https://doi.org/10.1016/j.cej.2011.05.012
36. K. Singh, D.H. Lataye and K.L. Wasewar, *J. Hazard. Toxic Radioact. Waste*, **20**, 04015024 (2016); https://doi.org/10.1061/(ASCE)HZ.2153-5515.0000309
37. R. Araga, S. Soni and C.S. Sharma, *J. Environ. Chem. Eng.*, **5**, 5608 (2017); https://doi.org/10.1016/j.jece.2017.10.023
38. K. Singh, D.H. Lataye and K.L. Wasewar, *J. Fluor. Chem.*, **194**, 23 (2017); https://doi.org/10.1016/j.jfluchem.2016.12.009
39. E.K. Guechi and O. Hamdaoui, *Desalination Water Treat.*, **57**, 10677 (2016); https://doi.org/10.1080/19443994.2015.1038739
40. A.M. George and A. Tembhurkar, *Sustain. Chem. Pharm.*, **10**, 125 (2018); https://doi.org/10.1016/j.scp.2018.10.007
41. D. Srinivasulu and P.K. Pindi, *Water Sci. Technol. Water Supply*, **21**, 1594 (2021); https://doi.org/10.2166/ws.2021.037
42. S. Sihag and J. Pal, *Adv. Environ. Technol.*, **9**, 194 (2023); https://doi.org/10.22104/aet.2023.5963.1643